Hindawi Publishing Corporation
VLSI Design
Volume 2013, Article ID 738057, 9 pages
http://dx.doi.org/10.1155/2013/738057

Research Article

Discrete Wavelet Transform on Color Picture Interpolation of Digital Still Camera

Yu-Cheng Fan and Yi-Feng Chiang

Department of Electronic Engineering and Graduate Institute of Computer and Communication Engineering, National Taipei University of Technology, 1, Section 3, Chung-Hsiao East Road, Taipei 10608, Taiwan

Correspondence should be addressed to Yu-Cheng Fan; skystarfan@ntu.edu.tw and Yi-Feng Chiang; arvinchiang0@gmail.com

Received 5 October 2012; Accepted 18 January 2013

Academic Editor: Yeong-Kang Lai

Many people use digital still cameras to take photographs in contemporary society. Significant amounts of digital information have led to the emergence of a digital era. Because of the small size and low cost of the product hardware, most image sensors use a color filter array to obtain image information. However, employing a color filter array results in the loss of image information; thus, a color interpolation technique must be employed to retrieve the original picture. Numerous researchers have developed interpolation algorithms in response to various image problems. The method proposed in this study involves integrating discrete wavelet transform (DWT) into the interpolation algorithm. The method was developed based on edge weight and partial gain characteristics and uses the basic wavelet function to enhance the edge performance and processes of the nearest or larger and smaller direction gradients. The experiment results were compared to those of other methods to verify that the proposed method can improve image quality.

1. Introduction

The basic principles of digital still cameras and traditional cameras are analogous. Traditional cameras use sensitization negatives to sense the input image. Digital still cameras project the input image onto a charge-coupled device (CCD), where it is transformed into a digital signal. The digital signal is then stored in a memory component after compression. However, this signal indicates the light intensity and not the color variation. Therefore, a color filter array must be employed for digital sampling. Color filter arrays typically employ the RGB original color separation technique, where red, green, and blue values are mixed into a complete color image after the original image is passed through three color filter arrays. Because of the high costs and large space required to use three color filter arrays with CCDs, only one color filter array with a CCD is employed. Consequently, each pixel possesses only one red, green, and blue color elements. The general color filter array in digital still cameras possesses a Bayer pattern [1], as shown in Figure 1. An interpolation algorithm must be employed to identify the two missing colors based on the surrounding pixels. The zipper effect or false colors are typically observed in images after interpolation. Numerous interpolation algorithms have been proposed to resolve these problems and obtain good image quality.

Image interpolation methods possess spatial and frequency characteristics. Edge direction and nonedge direction interpolation methods adopt spatial characteristics. The adjacent pixels selected by nonedge direction interpolation methods are constant. Examples of this method type include the bilinear interpolation method [2] and color difference interpolation method [3]. Because these methods do not detect edges, the edges of partial images are blurred following interpolation. The adjacent pixels selected by edge direction interpolation methods are nonconstant. These methods can detect and reduce blurred edges in the horizontal and vertical directions of an image. Examples of this method type include the edge sensing interpolation method [4] and edge correlation sensing correction interpolation method [5]. Frequency characteristic interpolation methods include the alternating

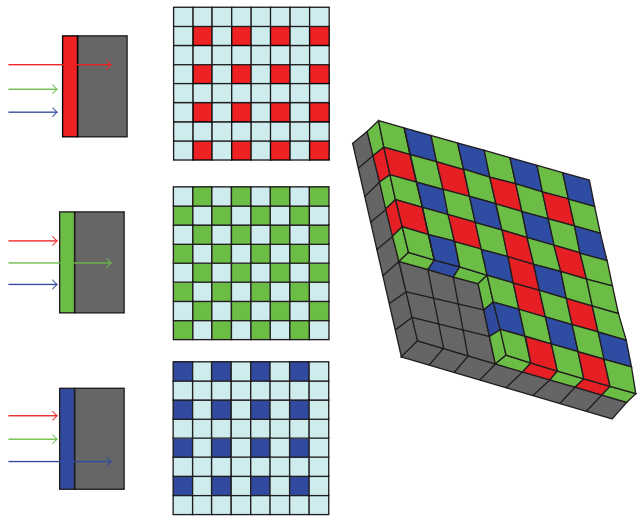

Figure 1: Bayer pattern color filter array.

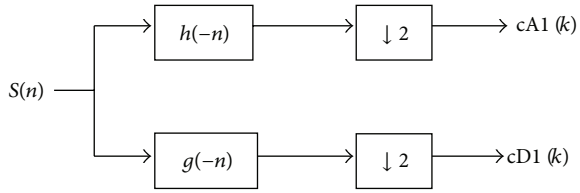

Figure 2: First-order wavelet transform decomposition.

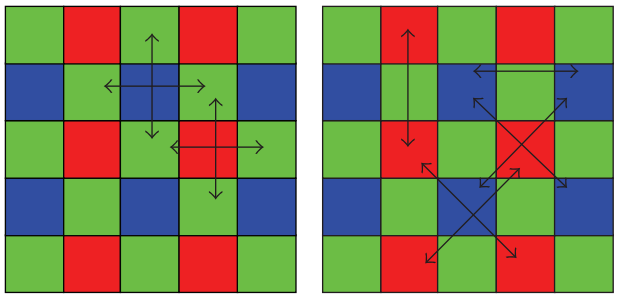

Figure 3: (a) Green interpolation and (b) red or blue interpolation.

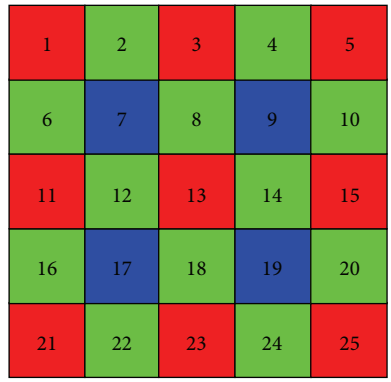

Figure 4: Interpolation reference.

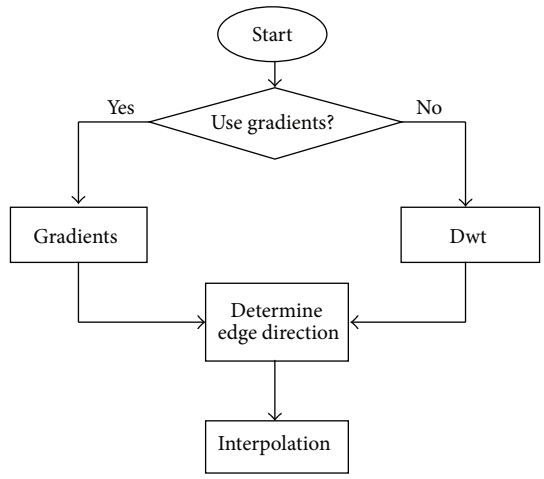

Figure 5: Flowchart of the processes in Algorithm 1.

projections interpolation method [6] and novel frequency-domain interpolation method [7]. Interpolation methods of this type use high- or low-frequency correlation to improve image aliasing and contrived phenomena and can provide high-quality images. A number of studies have employed a combination of the described methods or have proposed methods that use a wavelet algorithm for the edge or frequency domains [8–10]. Common research techniques are based on the physical characteristics of interference [11, 12]. Furthermore, the method combines edge and frequency algorithms for interpolation [13–15]. In [12], good missing green samples were first obtained based on the variances of color differences along a correct edge direction. The red and blue components were then interpolated based on the interpolated green plane. The refinement scheme was employed

```
if (|(G8-G18)|>0)&(|(G12-G14)|>0)···
    &(|(G8-G18)|<Thd)&(|(G12-G14)|<Thd)···
    &(|(G8-G18)|>0&|(G8-G12)|>0&|(G8-G14)|>0)
    cD1H=|(G8-G18)|+|(R13*2 -R3-R23)|;
    cD2V=|(G12-G14)|+|(R13*2-R11-R15)|;
else
    [cA1, cD1]=DWT(G8, G18);
    [cA2, cD2]=DWT(G12, G14);
    cD1H=|(cD1(2:2))|+|(R13*2-R3-R23)|;
    cD2V=|(cD2(2:2))|+|(R13*2-R11-R15)|;
end
if (cD2V>cD1H)
    G13=(G8+G18)/2+(R13*2-R3-R23)/4;
elseif (cD1H>cD2V)
    G13=(G12+G14)/2+(R13*2-R11-R15)/4;
else
    G13=(G8+G18+G12+G14)/4;
end
```

Algorithm 1

```
if (|(B7-B19)|<Thd1&|(B7-B17)|<Thd1&|(B7-B9)|<Thd1)
    [cA1, cD1]=DWT(B7, B19);
    [cA2, cD2]=DWT(B17, B9);
    cD1H=|(cD1(2:2))|;
    cD2V=|(cD2(2:2))|;
    if cD1H<cD2V
        B13=G13+(B7-G7+B19-G19)/2;
    elseif cD1H>cD2V
        B13=G13+(B9-G9+B17-G17)/2;
    else
        B13=G13+(B7-G7+B19-G19+B9-G9+B17-G17)/4;
    end
else
    B13=G13+(B7-G7+B19-G19+B9-G9+B17-G17)/4;
end
```

Algorithm 2

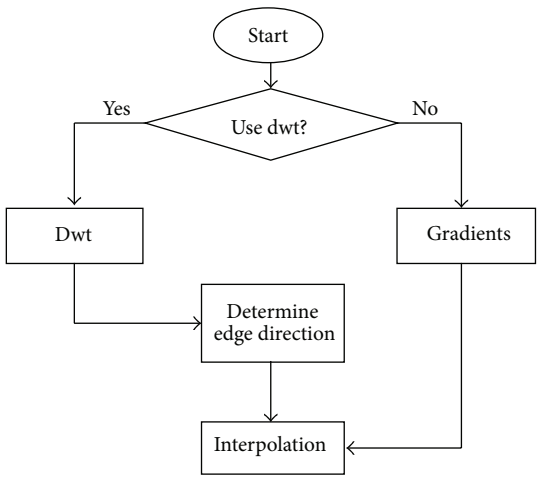

Figure 6: Flowchart of the processes in Algorithm 2.

Table 1: Peak signal-to-noise ratio (unit: dB).

thd (thd1 = 1)	R	G	B	Average
50	37.6492	39.2368	37.7998	38.2286
100	37.6681	39.2605	37.8147	38.2478
150	37.6753	39.2719	37.8249	38.2574
200	37.6745	39.2742	37.8265	38.2584
210	37.6745	39.2742	37.8265	38.2584
220	37.6745	39.2742	37.8265	38.2584
221	37.6745	39.2742	37.8265	38.2584
222	37.6745	39.2742	37.8265	38.2584
223	37.6745	39.2742	37.8265	38.2584
224	37.6745	39.2742	37.8265	38.2584
225	37.6745	39.2742	37.8265	38.2584
230	37.6730	39.2722	37.8267	38.2573
240	37.6730	39.2722	37.8267	38.2573
250	37.6730	39.2722	37.8267	38.2573

Table 2: Peak signal-to-noise ratio (unit: dB).

thd 1 (thd = 223)	R	G	B	Average
1	37.6745	39.2742	37.8265	38.2584
2	37.6745	39.2742	37.8265	38.2584
3	37.6742	39.2742	37.8261	38.2582
4	37.6734	39.2742	37.8252	38.2576
5	37.6719	39.2742	37.8239	38.2567
10	37.6597	39.2742	37.8091	38.2477
20	37.6127	39.2742	37.7594	38.2154
30	37.5647	39.2742	37.7081	38.1823
40	37.5103	39.2742	37.6582	38.1476
50	37.4765	39.2742	37.6223	38.1243
100	37.4035	39.2742	37.5498	38.0758
150	37.3927	39.2742	37.5365	38.0678
200	37.3926	39.2742	37.5357	38.0675
250	37.3923	39.2742	37.5346	38.0670

to improve the interpolation performance. The method employed in [15] obtains luminance values at the green sample locations and preserves high-frequency information. An adaptive filter was used to estimate the luminance values of the red and blue samples. Then, the estimated full-resolution luminance was used to interpolate the red, green, and blue color components. These results indicate that many interpolation methods result in contrived colors or blurred edges because they cannot sensitively detect edges or perform appropriate color interpolation. Therefore, effective interpolation of the image edge cannot be achieved. In this study, the relationship between the surrounding interpolation pixel weights and discrete wavelet transform (DWT) was used to perform color interpolation and edge detection. The results

Figure 7: Standard images.

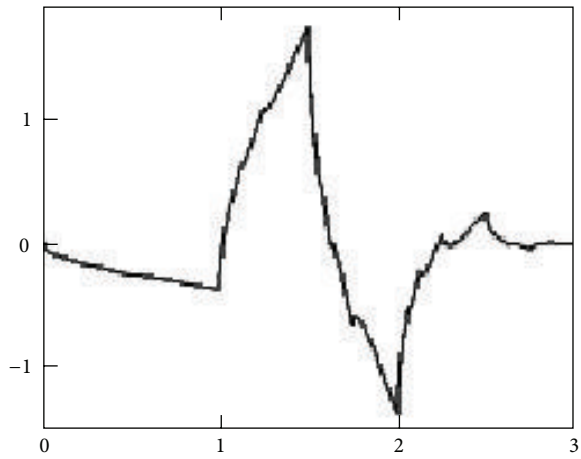

Figure 8: db2 wavelet waveform.

were then compared with those reported by other studies using conventional methods.

2. Proposed Method and DWT

2.1. Discrete Wavelet Transform. DWT can use the basic wavelet function $\phi(t)$ and scaling function $\psi(t)$ to conduct decomposition and reconstruction of sampling signals. The basic function is used to detect detailed variations. The scaling function is used to approximate original signals, which can be denoted as

$$\psi(t) = \sum_n g(n)\sqrt{2}\phi(2t-n),$$
$$\phi(t) = \sum_n h(n)\sqrt{2}\phi(2t-n). \quad (1)$$

Table 3: Peak signal-to-noise ratio comparison (unit: dB).

Studies	Sakamoto et al. [2]	Gunturk et al. [6]	Pei and Tam [3]	Dubois [7]	Lukac et al. [5]	Chung et al. [13]	Proposed
Picture 01	30.85	38.05	34.08	38.02	37.41	**39.88**	38.26
Picture 02	36.03	37.55	35.54	37.88	37.78	37.96	**38.96**
Picture 03	35.88	42.06	39.78	42.17	42.32	42.91	**43.70**
Picture 04	28.62	34.73	31.57	35.13	34.29	**36.22**	34.62
Picture 05	35.60	41.75	39.36	41.71	41.59	42.05	**43.09**
Picture 06	32.57	39.22	36.06	38.86	38.74	**40.17**	39.72
Picture 07	36.03	39.07	39.16	39.32	40.01	39.79	**41.92**
Picture 08	32.00	37.94	35.25	39.96	37.45	**40.75**	39.19
Picture 09	35.76	42.11	40.29	42.17	42.19	42.32	**43.35**
Picture 10	33.13	35.89	35.93	36.04	37.07	36.24	**39.28**
Picture 11	32.30	37.39	35.43	37.27	37.09	37.68	**38.27**
Picture 12	34.21	37.93	36.93	38.22	38.52	38.45	**40.80**
Picture 13	36.73	41.45	41.23	41.69	42.39	42.31	**43.25**
Picture 14	36.36	41.57	40.72	41.97	42.48	41.67	**43.96**
Picture 15	33.36	39.31	37.86	39.81	39.14	**40.56**	40.41
Picture 16	35.02	38.94	38.92	39.27	39.25	39.33	**40.91**
Picture 17	32.50	40.38	35.51	40.42	39.34	41.75	**41.98**
Picture 18	37.75	41.71	42.12	42.19	42.93	42.07	**43.73**
Picture 19	36.51	40.38	39.94	40.52	40.79	40.15	**42.66**
Picture 20	28.59	37.26	31.04	35.27	34.57	**37.56**	36.76
Picture 21	36.34	42.52	40.33	42.98	42.27	43.54	**44.55**
Picture 22	34.83	42.10	38.32	43.71	40.45	**44.31**	41.63
Picture 23	33.03	40.83	38.99	40.39	41.18	**41.58**	40.80
Picture 24	30.66	34.92	33.95	35.34	34.89	35.29	**36.46**
Average	33.94	39.38	37.43	39.60	39.34	40.19	**40.76**

The basic wavelet function can be calculated from the scaling function. $g(n)$ and $h(n)$ are digital filter coefficients; their relationship is expressed as

$$g(n) = (-1)^n h(l - n - 1). \tag{2}$$

In wavelet transform, $g(n)$ and $h(n)$ are approximately equal to a high-pass filter and a low-pass filter. In (2), l denotes the filter length. DWT has a similar function as a filter and can analyze the signal layer by layer. This filter comprises a high-pass filter and a low-pass filter. Figure 2 shows the operational manner and first-order wavelet transform decomposition of this filter. cA1(k) is an approximate coefficient. This indicates that the signal passes through a low-pass filter and undergoes downsampling. Approximate coefficients retain low-frequency information of the original signal $S(n)$ and less high-frequency noise. cD1(k) is a detailed coefficient. This indicates that the signal passes through a high-pass filter and undergoes downsampling. Detailed coefficients retain high-frequency information of the original signal $S(n)$. Figure 2 is used in $\downarrow 2$ to denote downsampling, which involves retaining half low-frequency and half high-frequency data. The method involves sampling odd and even terms.

The wavelet transform decomposition process is expressed as

$$\begin{aligned} \text{cA1}(k) &= \sum_n h(n - 2k) S(n) \\ \text{cD1}(k) &= \sum_n g(n - 2k) S(n). \end{aligned} \tag{3}$$

2.2. Proposed Method. Image information is obtained after passing through a Bayer pattern color filter array. Horizontal and vertical direction information is used to interpolate the green portion. For the red and blue portions, only information in the horizontal, vertical, and diagonal directions can be employed, as shown in Figure 3. Therefore, in this study, the wavelet sensitivity and color correlation weight [4] are used to identify the horizontal, vertical, and/or diagonal directions and interpolate missing pixels.

Please refer to Figure 4. The green interpolation method can be expressed asshown in Algorithm 1.

cD1H is the horizontal gradient. cD2V is the vertical gradient. Thd is determined through an experiment and is used to limit the range of the nearest or smaller direction gradients. When the horizontal or vertical gradients are small,

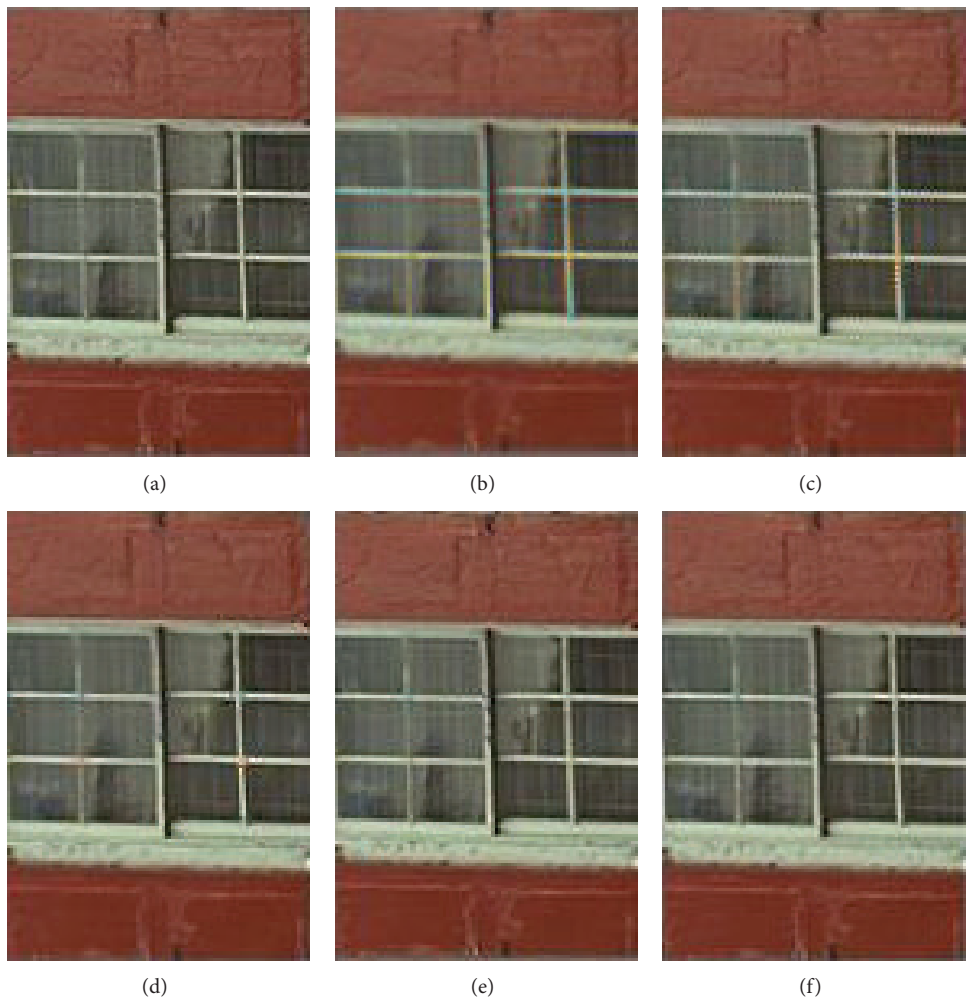

Figure 9: (a) Original picture, (b) bilinear interpolation, (c) color difference interpolation, (d) edge detection interpolation, (e) adaptive color plane interpolation, and (f) the proposed method.

DWT is used to detect edges and is judged according to gradients. Because of the good sensitivity of DWT, detailed coefficients cD1 and cD2 can be obtained to enhance the gradients. If an edge exists, it has the correct cD1 or cD2 to determine the edge direction. G8 and G18 are calculated by DWT, which produces cA1 and cD1. G12 and G14 follow the same procedure. Figure 5 shows the flowchart of the processes in Algorithm 1. First, the operations were assessed, the edge direction was determined, and then interpolation was conducted.

Please refer to Figure 4. The red and blue interpolation methods can be expressed as shown in Algorithm 2.

When the gradients are relatively close, DWT is used to detect edges; otherwise, the color correlations are employed to interpolate directly. Thd1 is determined through an experiment. Furthermore, the edge direction of large gradients can be adjusted to limit the range of the nearest or larger direction gradients. Figure 6 shows a flowchart of the processes in Algorithm 2. First, the operations are assessed. If DWT is employed, the edge direction is determined before conducting interpolation; otherwise, interpolation is directly performed. The horizontal and vertical directions only possess information of the two adjacent pixels; thus, their correlation is directly employed for interpolation. The interpolation method can be expressed as

$$B8 = G8 + \frac{(B7 - G7 + B9 - G9)}{2}. \quad (4)$$

The green interpolation method is identical to the red and blue interpolation methods. Diagonal interpolation of red and blue follows the same method used for blue and red. Furthermore, the red horizontal or vertical interpolation method is identical to that of blue.

3. Simulation Result

This study employed 24 standard color pictures provided for popular use. These images measure 512 × 768 or 768 × 512, as shown in Figure 7, and have been included in numerous studies. To begin the simulation, raw image data are read and then separated into red, blue, and green image planes before sampling using the Bayer pattern. Regarding wavelet function

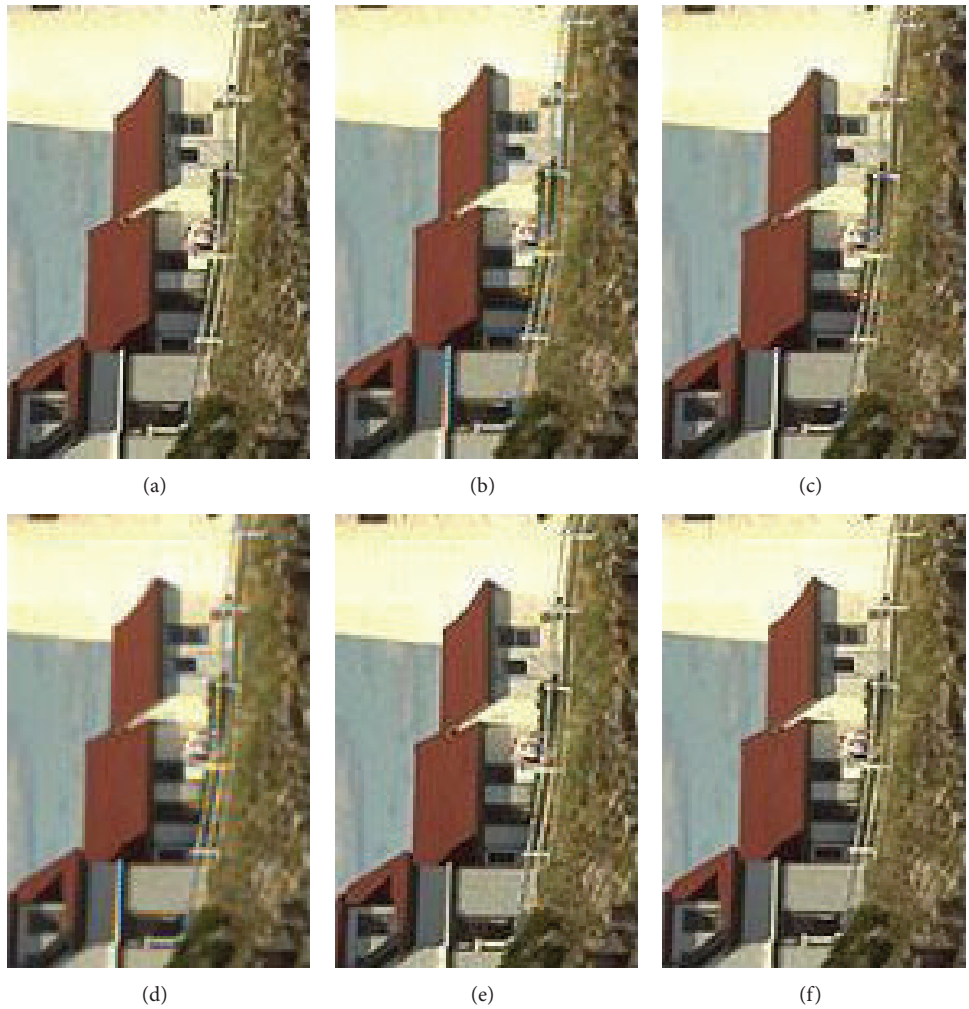

Figure 10: (a) Original picture, (b) bilinear interpolation, (c) color difference interpolation, (d) edge detection interpolation, (e) adaptive color plane interpolation, and (f) the proposed method.

selection, for this study, we adopted Daubechies wavelets for the basic functions and used the db2 function for simulation. Db2 is a second-rank Daubechies wavelet with a filter length of 4 and four low-pass filter coefficients denoted as $h0$, $h1$, $h2$, and $h3$. The values of these coefficients are 0.34151, 0.59151, 0.15849, and −0.091506. Employing the db2 wavelet for simulation provides the optimum result. Db2 to db7 were analyzed using, which indicated that shorter filters provide superior results. Furthermore, only one transformation is required. When transformed numerous times, waveforms are stretched to the left and right. Figure 8 shows a db2 wavelet waveform. Wavelet waveforms and filter coefficients are closely linked. Employing the adaptive wavelet function to analyze signals provides superior results. The waveform compression and stretch characteristics provide superior results in the shortest time variations and can be understood through observation. According to the experiment results, Thd and Thd1 were 223 and 1, respectively. The experimental process is shown in Tables 1 and 2. Picture 01 was used as an example. Furthermore, 223 and 1 were the stable range values.

Table 3 shows a comparison of the peak signal-to-noise ratio (PSNR) in this study with that of other studies. The organizational sequence for the standard images in Figure 7 was from left to right and top to bottom. These images were named according to a nominal scale as Picture 01 to Picture 24. After processing, the images differ from their original appearance. To examine the image quality, PSNR is typically contrasted. PSNR can be expressed as

$$\mathrm{MSE} = \frac{1}{mn}\sum_{i=0}^{m-1}\sum_{j=0}^{n-1}\left[I(i,j) - K(i,j)\right]^2,$$
$$\mathrm{PSNR} = 10\cdot\log_{10}\left(\frac{\mathrm{MAX}_I^2}{\mathrm{MSE}}\right) = 20\cdot\log_{10}\left(\frac{\mathrm{MAX}_1}{\sqrt{\mathrm{MSE}}}\right). \quad (5)$$

$I(i, j)$ of the mean square error (MSE) is the pixel value of the original image and is located at (i, j). $P(i, j)$ is the pixel value of position (i, j) after image processing. The unit of PSNR is in decibels (dB). A larger PSNR indicates less aliasing. MAX_I denotes the largest image pixel color value. If 8 bits are used to represent each sample pixel, the total bit

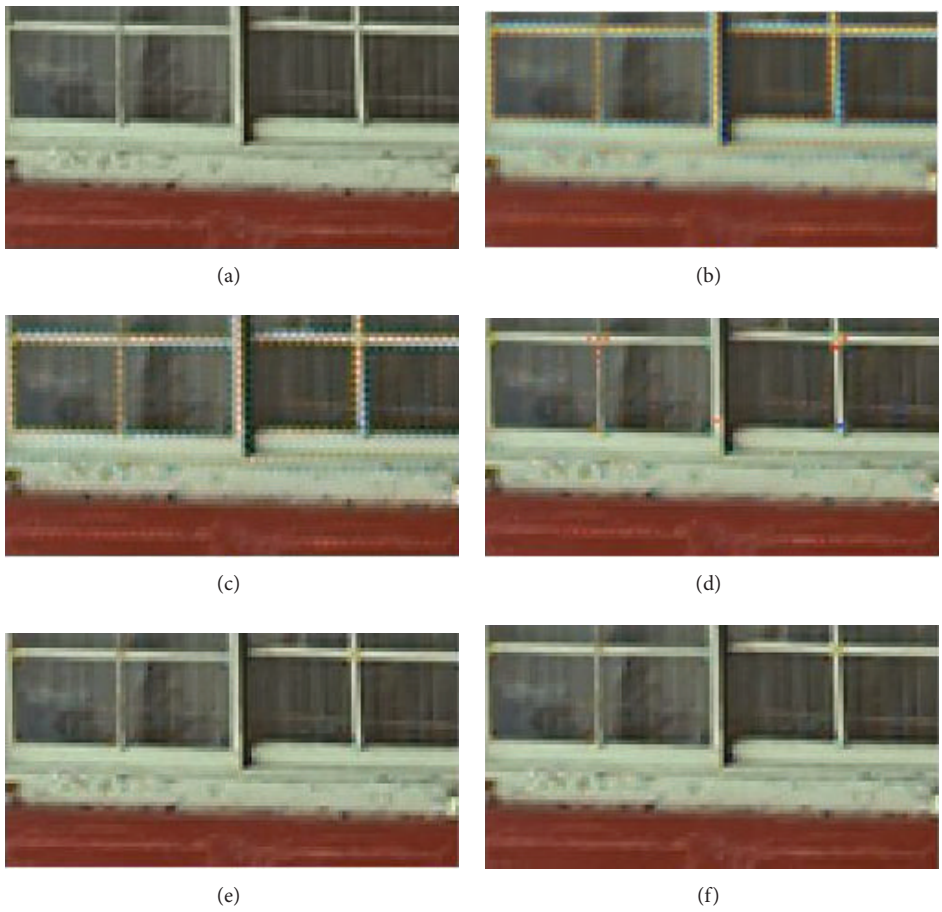

(a) (b) (c) (d) (e) (f)

Figure 11: (a) Original picture, (b) bilinear interpolation, (c) color difference interpolation, (d) edge detection interpolation, (e) adaptive color plane interpolation, and (f) the proposed method.

number is 255. The results in Table 3 show that the proposed method provides a superior image quality compared to that in previous studies. Most images have large low-frequency areas. Thus, the spatial domain interpolation algorithm can be used to process most of images. However, if images possess a large fluid wave, wood, or grassy area, similar to Picture 22, the frequency domain algorithm provides a superior performance. Table 4 shows a PSNR evaluation, including each RGB color component and their average.

Figures 9 and 10 show Pictures 1 and 6, respectively. These images were selected from among the 24 standard images. The proposed method and conventional interpolation methods were used for simulation. Magnifying the images shows that the proposed method improves image quality significantly, as shown in Figure 11.

The images processed by using the proposed method are extremely similar to the original images. Figure 11 shows a magnification of Figure 9. DWT exhibited good edge detection sensitivity and partially resolved the zipper effects, color shifts, aliasing artifacts, blur effects, and obvious unnatural color grains. Furthermore, DWT limited the unnatural colors of the window lattice and the color inaccuracies of the crisscross.

4. Conclusion

Science and technology change every day. Although chip processing speeds continue to accelerate, their size and costs are increasingly decreasing. The proposed method does not employ frequency characteristics; instead, image quality is enhanced using spatial characteristics. Previous studies have discussed the importance of edges and interpolation pixels and calculated the frequency and spatial characteristics. This study exploited the sensitivity of wavelet algorithms and the correlation between colors to obtain good results regarding image edges and interpolation pixels. Comparing the simulation results to those of previous studies, the experimental images and data indicate that the proposed method can provide high-quality images.

Conflict of Interests

The authors do not have a direct financial relation with the commercial identity (Kodak Company and MATLAB/TOOLBOX) mentioned in our paper that might lead to a conflict of interests for any of the authors.

Table 4: Peak signal-to-noise ratio (unit: dB).

	R	G	B	Average
Picture 01	37.6746	39.2743	37.8266	38.2585
Picture 02	38.4116	39.9794	38.4853	38.9588
Picture 03	43.3799	45.1411	42.5881	43.7030
Picture 04	34.4073	35.2576	34.1865	34.6171
Picture 05	43.0901	44.0063	42.1758	43.0907
Picture 06	39.3456	40.6480	39.1629	39.7188
Picture 07	40.0361	44.1844	41.5367	41.9191
Picture 08	38.7940	40.3259	38.4501	39.1900
Picture 09	42.8313	44.7694	42.4572	43.3526
Picture 10	37.8463	41.1899	38.8066	39.2809
Picture 11	38.1024	39.1079	37.6140	38.2748
Picture 12	39.4213	42.0331	40.9348	40.7964
Picture 13	42.7354	45.0743	41.9345	43.2481
Picture 14	43.0495	45.4716	43.3727	43.9646
Picture 15	39.3880	41.5611	40.2815	40.4102
Picture 16	39.4140	42.9145	40.4108	40.9131
Picture 17	41.4268	42.9398	41.5827	41.9831
Picture 18	42.5319	45.8168	42.8554	43.7347
Picture 19	41.5696	44.2054	42.2152	42.6634
Picture 20	36.1300	37.8601	36.2973	36.7625
Picture 21	43.4639	45.9502	44.2462	44.5534
Picture 22	41.4209	43.0842	40.3746	41.6266
Picture 23	39.7628	42.0993	40.5352	40.7991
Picture 24	36.2665	37.6725	35.4316	36.4569
Average	40.02083	42.10696	40.15676	40.7615

Acknowledgments

This study was supported by the Taiwan e-learning and Digital Archives Program (TELDAP) and the National Science Council of Taiwan under Grant no. NSC 100-2631-H-027-003. The authors gratefully acknowledge the Chip Implementation Center (CIC) for supplying the technology models used for IC design.

References

[1] B. E. Bayer, "Color imaging array," U.S. Patent 3 971 065, 1976.

[2] T. Sakamoto, C. Nakanishi, and T. Hase, "Software pixel interpolation for digital still cameras suitable for a 32-bit MCU," *IEEE Transactions on Consumer Electronics*, vol. 44, no. 4, pp. 1342–1352, 1998.

[3] S. C. Pei and I. K. Tam, "Effective color interpolation in CCD color filter arrays using signal correlation," *IEEE Transactions on Circuits and Systems for Video Technology*, vol. 13, no. 6, pp. 503–513, 2003.

[4] J. E. Adams Jr., "Design of practical color filter array interpolation algorithms for digital cameras," in *2nd Real-Time Imaging*, vol. 3028 of *Proceedings of SPIE*, pp. 117–125, February 1997.

[5] R. Lukac, K. N. Plataniotis, D. Hatzinakos, and M. Aleksic, "A new CFA interpolation framework," *Signal Processing*, vol. 86, no. 7, pp. 1559–1579, 2006.

[6] B. K. Gunturk, Y. Altunbasak, and R. M. Mersereau, "Color plane interpolation using alternating projections," *IEEE Transactions on Image Processing*, vol. 11, no. 9, pp. 997–1013, 2002.

[7] E. Dubois, "Frequency-domain methods for demosaicking of bayer-sampled color images," *IEEE Signal Processing Letters*, vol. 12, no. 12, pp. 847–850, 2005.

[8] B. G. Jeong, S. H. Hyun, and I. K. Eom, "Edge adaptive demosaicking in wavelet domain," in *Proceedings of the 9th International Conference on Signal Processing (ICSP'08)*, pp. 836–839, Beijing, China, October 2008.

[9] L. Chen, K. H. Yap, and Y. He, "Color filter array demosaicking using wavelet-based subband synthesis," in *Proceedings of the IEEE International Conference on Image Processing (ICIP'05)*, pp. II-1002–II-1005, September 2005.

[10] J. Driesen and P. Scheunders, "Wavelet-based color filter array demosaicking," in *Proceedings of the International Conference on Image Processing (ICIP'04)*, vol. 5, pp. 3311–3314, October 2004.

[11] X. Wu and X. Zhang, "Joint color decrosstalk and demosaicking for CFA cameras," *IEEE Transactions on Image Processing*, vol. 19, no. 12, pp. 3181–3189, 2010.

[12] K. H. Chung and Y. H. Chan, "Color demosaicing using variance of color differences," *IEEE Transactions on Image Processing*, vol. 15, no. 10, pp. 2944–2955, 2006.

[13] K. L. Chung, W. J. Yang, W. M. Yan, and C. C. Wang, "Demosaicing of color filter array captured images using gradient edge detection masks and adaptive heterogeneity-projection," *IEEE Transactions on Image Processing*, vol. 17, no. 12, pp. 2356–2367, 2008.

[14] K. L. Chung, W. J. Yang, P. Y. Chen, W. M. Yan, and C. S. Fuh, "New joint demosaicing and zooming algorithm for color filter array," *IEEE Transactions on Consumer Electronics*, vol. 55, no. 3, pp. 1477–1486, 2009.

[15] N. X. Lian, L. Chang, Y. P. Tan, and V. Zagorodnov, "Adaptive filtering for color filter array demosaicking," *IEEE Transactions on Image Processing*, vol. 16, no. 10, pp. 2515–2525, 2007.